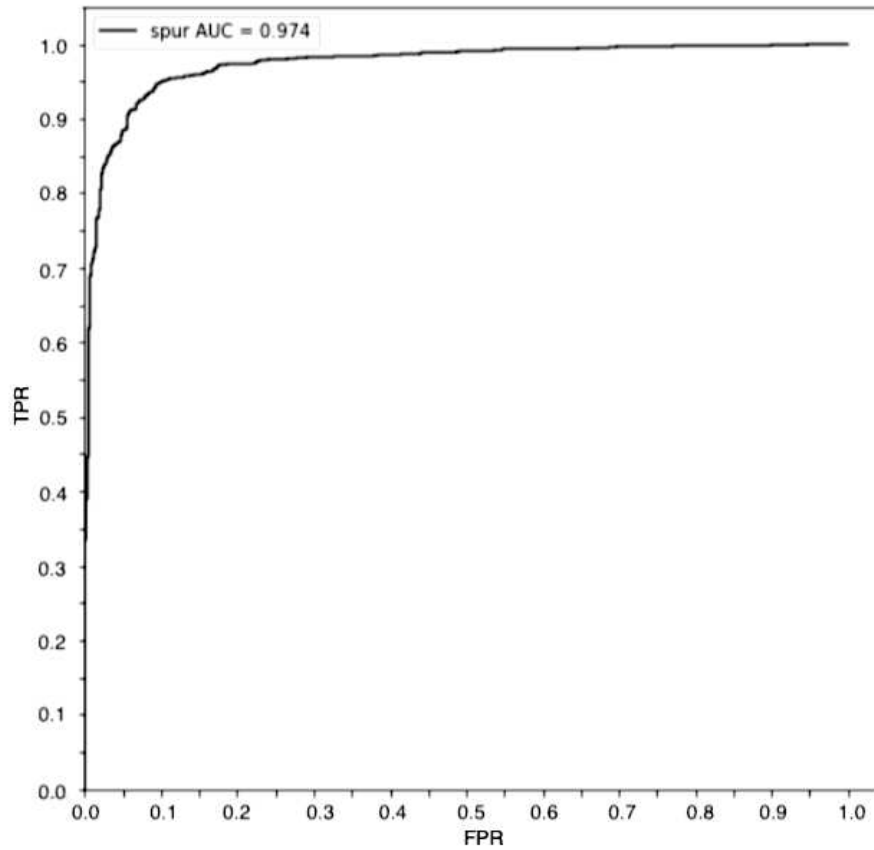
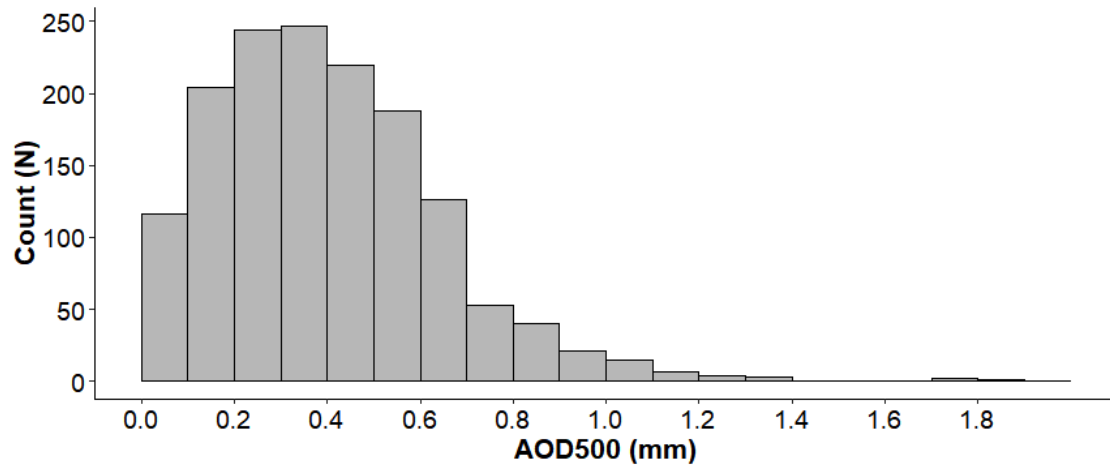


**Supplementary Figure 1.** Receiver operating characteristic (ROC) curve for scleral spur prediction by the DL algorithm in Heidelberg Engineering's internal test dataset.



TPR, True Positive Rate. FPR, False Positive Rate. AUC, Area Under Curve.

**Supplementary Figure 2.** Distribution of AOD500 as measured by the Reference Grader.



AOD500, Anterior Opening Distance 500  $\mu$ m from the scleral spur.

**Supplementary Table 1.** Intraclass correlation coefficients (ICCs) with 95% confidence intervals comparing measurements from the superior sector by the Reference Grader and a second human grader or DL algorithm.

	<b>Expert Grader</b>	<b>Novice Grader</b>	<b>FPR4</b>	<b>TPR95</b>
<b>ACW</b>	0.891 (0.743 - 0.956)	0.531 (0.095 - 0.799)	0.970 (0.903 - 0.991)	0.956 (0.889 - 0.983)
<b>LV</b>	0.996 (0.988 - 0.998)	0.990 (0.972 - 0.997)	0.998 (0.993 - 0.999)	0.996 (0.990 - 0.999)
<b>AOD500</b>	0.981 (0.961 - 0.991)	0.907 (0.808 - 0.956)	0.989 (0.976 - 0.995)	0.986 (0.971 - 0.993)
<b>AOD750</b>	0.970 (0.939 - 0.986)	0.950 (0.897 - 0.977)	0.994 (0.987 - 0.997)	0.975 (0.950 - 0.988)
<b>TISA500</b>	0.957 (0.908 - 0.980)	0.782 (0.557 - 0.901)	0.976 (0.944 - 0.990)	0.946 (0.882 - 0.976)
<b>TISA750</b>	0.97 (0.934 - 0.986)	0.871 (0.723 - 0.943)	0.985 (0.965 - 0.994)	0.962 (0.916 - 0.983)
<b>SSA500</b>	0.976 (0.95 - 0.989)	0.925 (0.843 - 0.965)	0.983 (0.963 - 0.993)	0.978 (0.953 - 0.989)
<b>SSA750</b>	0.961 (0.921 - 0.981)	0.946 (0.887 - 0.974)	0.99 (0.979 - 0.996)	0.97 (0.939 - 0.986)

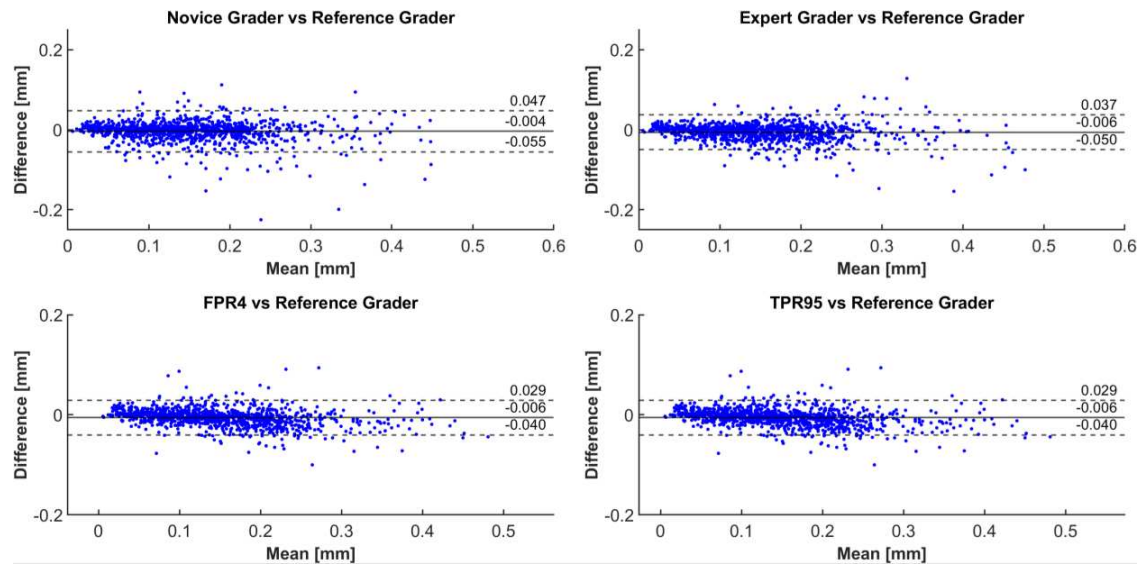
ACW, Anterior Chamber Width. LV, Lens Vault. AOD500/750, Anterior Opening Distance 500/750  $\mu\text{m}$  from the scleral spur. TISA500/750, Trabecular Iris Space Area 500/750  $\mu\text{m}$  from the scleral spur. SSA500/750, Scleral Spur Angle 500/750  $\mu\text{m}$  from the scleral spur.

**Supplementary Table 2.** Intraclass correlation coefficients (ICCs) with 95% confidence intervals comparing measurements from the temporal sector by the Reference Grader and a second human grader or DL algorithm.

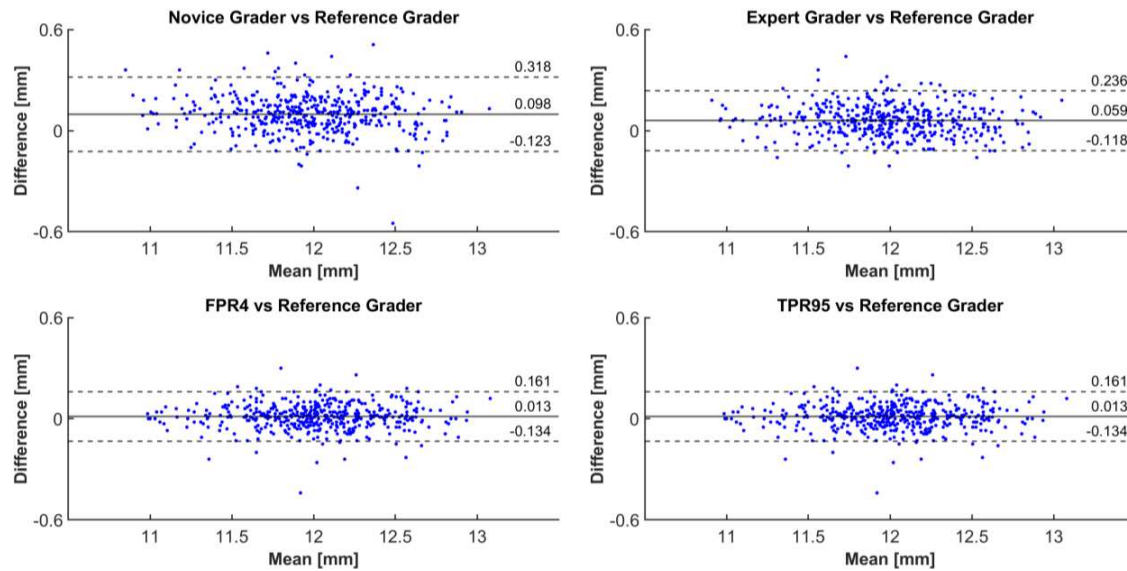
	<b>Expert Grader</b>	<b>Novice Grader</b>	<b>FPR4</b>	<b>TPR95</b>
<b>ACW</b>	0.955 (0.942 - 0.966)	0.927 (0.905 - 0.943)	0.980 (0.973 - 0.985)	0.978 (0.971 - 0.983)
<b>LV</b>	0.996 (0.994 - 0.997)	0.994 (0.993 - 0.996)	0.996 (0.995 - 0.997)	0.996 (0.995 - 0.997)
<b>AOD500</b>	0.965 (0.955 - 0.973)	0.950 (0.936 - 0.962)	0.979 (0.972 - 0.984)	0.979 (0.972 - 0.984)
<b>AOD750</b>	0.977 (0.970 - 0.982)	0.969 (0.960 - 0.977)	0.984 (0.980 - 0.988)	0.984 (0.979 - 0.988)
<b>TISA500</b>	0.974 (0.965 - 0.981)	0.977 (0.969 - 0.983)	0.986 (0.981 - 0.990)	0.986 (0.981 - 0.990)
<b>TISA750</b>	0.981 (0.975 - 0.986)	0.978 (0.970 - 0.984)	0.988 (0.983 - 0.991)	0.988 (0.983 - 0.991)
<b>SSA500</b>	0.944 (0.927 - 0.957)	0.910 (0.884 - 0.931)	0.971 (0.962 - 0.978)	0.970 (0.961 - 0.977)
<b>SSA750</b>	0.964 (0.953 - 0.972)	0.942 (0.925 - 0.956)	0.983 (0.978 - 0.987)	0.982 (0.976 - 0.986)

ACW, Anterior Chamber Width. LV, Lens Vault. AOD500/750, Anterior Opening Distance 500/750  $\mu\text{m}$  from the scleral spur. TISA500/750, Trabecular Iris Space Area 500/750  $\mu\text{m}$  from the scleral spur. SSA500/750, Scleral Spur Angle 500/750  $\mu\text{m}$  from the scleral spur.

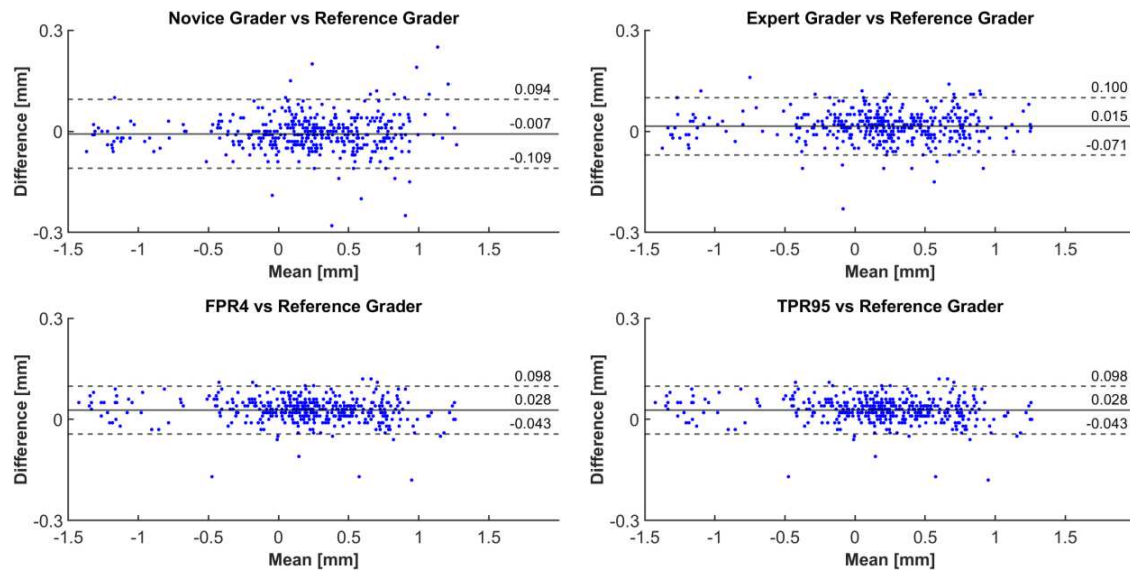
**Supplementary Figure 3.** Bland-Altman plots of human-human and human-machine comparisons of TISA500 measurements.



**Supplementary Figure 4.** Bland-Altman plots of human-human and human-machine comparisons of ACW measurements.



**Supplementary Figure 5.** Bland-Altman plots of human-human and human-machine comparisons of LV measurements.



**Supplementary Figure 6.** Representative cropped images of false positives (FP; top) and false negatives (FN; bottom) by the TPR95 algorithm based on the consensus between all three human graders. Red dots in FP images indicate predicted scleral spur location by TPR95 algorithm. Blue dots in FN images indicate scleral spur location marked by the Reference Grader.

